

Sensitivity of coherent oscillations in rat hippocampus to AC electric fields

Jacqueline K. Deans, Andrew D. Powell and John G. R. Jefferys

Department of Neurophysiology, Division of Neuroscience, Medical School, University of Birmingham, Edgbaston, Birmingham B15 2TT, UK

The sensitivity of brain tissue to weak extracellular electric fields is important in assessing potential public health risks of extremely low frequency (ELF) fields, and potential roles of endogenous fields in brain function. Here we determine the effect of applied electric fields on membrane potentials and coherent network oscillations. Applied DC electric fields change transmembrane potentials in CA3 pyramidal cell somata by 0.18 mV per $V\ m^{-1}$ applied. AC sinusoidal electric fields have smaller effects on transmembrane potentials: sensitivity drops as an exponential decay function of frequency. At 50 and 60 Hz it is ~ 0.4 that for DC fields. Effects of fields of $\leq 16\ V\ m^{-1}$ peak-to-peak (p-p) did not outlast application. Kainic acid (100 nM) induced coherent network oscillations in the beta and gamma bands (15–100 Hz). Applied fields of $\geq 6\ V\ m^{-1}$ p-p ($2.1\ V\ m^{-1}$ r.m.s.) shifted the gamma peak in the power spectrum to centre on the applied field frequency or a subharmonic. Statistically significant effects on the timing of pyramidal cell firing within the oscillation appeared at distinct thresholds: at 50 Hz, $1\ V\ m^{-1}$ p-p ($354\ mV\ m^{-1}$ r.m.s.) had statistically significant effects in 71% of slices, and $0.5\ V\ m^{-1}$ p-p ($177\ mV\ m^{-1}$ r.m.s.) in 20%. These threshold fields are consistent with current environmental guidelines. They correspond to changes in somatic potential of $\sim 70\ \mu V$, below membrane potential noise levels for neurons, demonstrating the emergent properties of neuronal networks can be more sensitive than measurable effects in single neurons.

(Resubmitted 31 May 2007; accepted after revision 21 June 2007; first published online 28 June 2007)

Corresponding author J. G. R. Jefferys: Department of Neurophysiology, Division of Neuroscience, Medical School, University of Birmingham, Edgbaston, Birmingham B15 2TT, UK. Email: j.g.r.jefferys@bham.ac.uk

The interaction of electric fields with neurons has implications both for the normal function of brain tissue, which can generate substantial fields during normal (Fujisawa *et al.* 2004) and pathological (Jefferys & Haas, 1982; Haas & Jefferys, 1984) activity, and for the concerns over health implications for people exposed to electromagnetic fields (Saunders & Jefferys, 2002).

The potential mechanisms for adverse effects of electromagnetic fields on neural tissue are not always obvious, but in the case of extremely low frequency fields (ELF, 1–300 Hz) modulation of membrane potential is the most likely. Previous studies on the hippocampal dentate gyrus and CA1 region *in vitro* revealed changes in neuronal responses with applied fields as weak as $0.3\text{--}10\ V\ m^{-1}$ (Jefferys, 1981; Bawin *et al.* 1986; Turner & Richardson, 1991; Lian *et al.* 2003; Francis *et al.* 2003; Fujisawa *et al.* 2004). Our work with DC fields applied to the CA1 region showed that the resulting changes in transmembrane potential had a time constant of several tens of milliseconds, which predicts that AC fields at powerline frequencies will have weaker effects (Bikson *et al.*

2004). However this work also suggested that there was no clear threshold, which raises the possibility that emergent properties of neuronal networks may be sensitive to AC fields that have effects below the noise levels of membrane potential, as long as they depend on the interactions of large numbers of neurons sharing common orientations with respect to the applied field. The emergent property we use in the present study is beta to gamma band (15–100 Hz) oscillations induced by bath applied kainic acid (Buhl *et al.* 1998; Vreugdenhil *et al.* 2003; Vreugdenhil & Toescu, 2005). This oscillation is generated in the CA3 region, particularly CA3c, and depends on synaptic interactions between pyramidal neurons and interneurons. Its origin in CA3 meant we needed to repeat our previous experiments on DC fields in this part of the hippocampus (Bikson *et al.* 2004) and to extend it to AC fields before measuring the impact on the coherent oscillations.

Methods

Slice preparation

Brain slices were prepared from adult male Sprague–Dawley rats (150–250 g; Charles River, UK). Animals were

This paper has online supplemental material.

anaesthetized with intraperitoneal ketamine (7.4 mg kg^{-1}) and medetomidine hydrochloride (0.7 mg kg^{-1}) prior to killing by cervical dislocation. The brain was quickly removed and placed into cold (3°C) sucrose cutting solution containing (mM): 189 sucrose, 2.5 KCl, 5 MgCl_2 , 1.2 NaH_2PO_4 , 26 NaHCO_3 , 0.1 CaCl_2 and 10 D-glucose pH 7.4, gassed with 95% O_2 –5% CO_2 . All procedures were regulated under the UK Animals (vibrating blade microtome, Scientific Procedures) Act 1986 and Institutional Ethics Committees.

Ventral slices of dorsal hippocampus, $400 \mu\text{m}$ thick, were prepared on an Integraslice (Campden Instruments, Loughborough, UK). After cutting, slices were placed in an interface recording chamber, perfused with artificial cerebrospinal fluid (aCSF) containing (mM): 125 NaCl, 3 KCl, 1.0 MgCl_2 , 1.25 NaH_2PO_4 , 26 NaHCO_3 , 2.0 CaCl_2 and 10 D-glucose, at pH 7.4, gassed with 95% O_2 –5% CO_2 . Osmolarity of the aCSF was $304 \text{ mosmol l}^{-1}$. Slices were allowed to recover for a period of 1 h prior to recording. Perfusion rates were 2 ml min^{-1} during recording of gamma oscillations and 1 ml min^{-1} during intracellular recording.

Application of currents

Chlorided silver electrodes 2 mm in diameter and 45 mm long were placed at the sides of the recording well $\sim 6 \text{ mm}$ from the slice and parallel to the flow of aCSF. Slices were positioned in the chamber so that the axis of the CA3c pyramidal cells' dendrites were parallel, and the pyramidal layer was perpendicular, to the direction of the applied electric field. The currents were generated by a constant current stimulator (model 2200, A-M Systems Inc, Carlsberg, WA, USA) under the control of DAC outputs from a Power1401 signal acquisition system (Cambridge Electronic Design Ltd (CED), Cambridge, UK). The waveforms were generated by Signal software (CED). At the start of each experiment we calibrated the applied current in terms of field strength using two electrodes placed 3 mm apart in the slice. Electric field strengths of 0.5, 1, 2, 3, 5, 10 and 16 V m^{-1} peak to peak (p-p; 0.177, 0.354, 0.708, 1.41, 2.12, 3.54 and 5.65 V m^{-1} r.m.s.) were tested in these experiments, using frequencies in the range 5–100 Hz, and durations of 1 s on, 1 s off for intracellular recordings and 10 s on, 30 s off for network oscillations. Fields at each frequency and strength were repeated five times and measurements averaged over the five repeats. Recordings confirmed that the field was uniform over most of the length of the recording chamber, and within the slices themselves (see online supplemental material Fig. 1).

Recording

Intracellular electrodes (60 – $120 \text{ M}\Omega$) were filled with 4 M potassium methylsulphate (Acros Organics, NJ, USA).

For intracellular recordings from CA3 pyramidal cell somata, the aCSF was supplemented with $20 \mu\text{M}$ NBQX, $25 \mu\text{M}$ D-APV (both Tocris, UK) and $10 \mu\text{M}$ bicuculline methiodide (Sigma, Gillingham, Dorset, UK) to prevent spontaneous synaptic potentials.

Extracellular network oscillations were recorded in area CA3c using borosilicate glass microelectrodes (GC120F-10, Clark Electromedical Instruments, Pangbourne UK). Electrodes were pulled with a Sutter P97 microelectrode puller (Sutter Instruments, Novato, CA, USA) and had DC resistances of 2–4 $\text{M}\Omega$ when filled with aCSF. Microelectrodes were connected to the recording circuit by a chlorided silver wire with a silver–silver chloride reference electrode placed in the bath near the aCSF outlet from the chamber. DC coupled signals were low-pass filtered at 2 kHz with an Axoprobe 1A (Axon Instruments, Union City, CA, USA) and Neurolog AC–DC amplifiers (Digitimer, Welwyn Garden City, UK); digitized at 5 kHz using a Power 1401 and Signal software (CED) and analysed off-line using Signal and Spike2 (CED).

Transmembrane potentials

Intracellular recordings are normally made with respect to a distant reference electrode in the bath. In the presence of significant potential gradients in the tissue and bath this configuration can lead to substantial errors in estimating the potential difference across the membrane, which is the value relevant to voltage-gated ion channels. We estimated transmembrane potential by subtracting the potential measured simultaneously at an extracellular microelectrode placed as close as possible to the intracellular recording microelectrode (see supplemental material Fig. 2). In order to avoid any errors due to voltage gradients over the few micrometres between the two microelectrodes, immediately after losing the cell we measured the voltage change induced by DC pulses with the previously intracellular electrode, and compared it with that measured by the extracellular electrode. This provided a correction factor that could be used to make small corrections to the calculation of transmembrane current. This normally was of the order of 1%, and we excluded recordings where the correction would have been greater than 2%.

Network oscillations

Network oscillations were generated by application of 100 nM kainic acid (Tocris, Bristol, UK) to the aCSF perfusing the slice. Beta–gamma oscillations (15–100 Hz) were observed within 10 min of kainic acid application. The peak frequency developed quickly and remained fairly constant throughout the 45 min development period.

The amplitude increased during the development period to stabilize after about 30 min of bath application. Application of electric fields started 45 min after kainic acid perfusion. The most common way of measuring such oscillations uses the fast Fourier transform (FFT) to generate power spectra. This was performed using Spike2 (CED). Where we wished to detect small differences in power spectra we calculated means and standard deviations of five repeats (unless stated otherwise) of the field application under each condition, and subtracted the mean spectra for the control condition from that during the applied fields. The standard deviations were pooled and doubled to provide a 95% confidence interval, which then could be plotted as error bars for the difference spectrum (SigmaPlot v. 8, Systat Software, London, UK). The entrainment of biological oscillations to the weaker applied fields was assessed by determining whether the distribution of the time differences between each cycle of the applied field and the spikes in the oscillations was uniform, which would be expected if there was no association. This used the Kolmogorov–Smirnov test for uniform distribution using SPSS for Windows v. 12 (SPSS UK Ltd, Woking, UK). In this case we identified the times of the small spikes within each cycle of the gamma oscillation using Spike2 to identify troughs in the data; the minima within the applied field were detected in the same way. In some cases we removed the applied sine wave from the raw data using the Spike2 script ‘remsin.exe’ available from <http://www.ced.co.uk/pru.shtml>, to avoid any risk of biasing the identification of troughs.

Epifluorescence measurement of field-induced changes in membrane potential

Epifluorescence measurement of field-induced changes in membrane potential used the fast-response voltage-sensitive dye RH-795 (Invitrogen, Paisley, UK). Slices were stained with 100 μM RH-795 (1 h at room temperature), and washed for ~ 10 min in aCSF before use.

Slices were placed submerged in a recording chamber and superfused (~ 4 ml min^{-1}) with warm (29–31°C) aCSF gassed with 95% O_2 –5% CO_2 . The slice was orientated so that the CA3c somato-dendritic axis was parallel to the direction of the applied electric field. Fields were applied using 12 mm long, 1 mm diameter sintered Ag–AgCl cylindrical pellet electrodes placed 4 mm apart. The electric field strength was calibrated as described above.

Epifluorescence measurements were made using a photomultiplier system (Cairn Research Ltd, Faversham, Kent, UK) mounted on an Olympus BX-51 upright microscope, fitted with an Olympus fluorplan 40 \times , 0.8 NA water immersion lens (Micro Instruments, Long Hanborough, UK). The fluorophore was excited with 520 ± 15 nm light using an Optoscan monochromator (Cairn Research Ltd).

Emitted light was detected by an S20 photomultiplier tube (Cairn Research Ltd) with an enhanced red response suitable for detection of wavelengths greater than 600 nm, and was sampled every 5 ms. Regions of interest were selected by use of rectangular field stops and were limited to a region of 50 μm^2 area of the objective field, centred around the CA3c pyramidal cell region.

In order to improve the signal-to-noise ratio, 100 traces were averaged for each region of interest. Fluorescence traces were corrected off-line for dye bleaching by subtraction of a control trace without applying electric fields. Light intensities were measured as relative fluorescence change ($\Delta F/F$), where F is the fluorescence intensity without stimulation and ΔF is the fluorescence change during field application.

Statistical analysis

Statistical analysis was performed using SPSS v. 12 for Windows, using tests cited in the text. Curve fitting was performed using SigmaPlot v. 8, which also produced the graphs.

Results

AC fields on CA3 pyramidal cells

Sinusoidal AC extracellular fields, with frequencies of 10–100 Hz, resulted in sinusoidal fluctuations in the somatic transmembrane potential at the same frequencies. Over the range of fields tested here (0.5–16.0 V m^{-1} p-p): the relationship between applied field and resulting change in transmembrane potential was linear (Fig. 1A), the intersection of the regression lines with the zero applied field did not differ significantly from the origin. The effects of applied fields in this range of strengths did not outlast their application (see supplemental material Fig. 3).

The relationship between transmembrane potential changes and applied AC fields at 10 Hz, at 0.21 ± 0.03 mV per V m^{-1} , did not differ significantly from that for DC fields, at 0.18 ± 0.04 mV per V m^{-1} . At higher frequencies the effects of the applied AC fields decreased substantially, dropping to 31% at 50 Hz and to 20% at 100 Hz (Fig. 1). Sample traces from one cell at 8 V m^{-1} p-p are shown above the graph of the pooled measurements (6 slices for each point). The relationship between the frequency of the applied field and the mean sensitivity of the transmembrane potential could be fitted with an exponential decay (Fig. 1; regression significant at $P < 0.0001$).

Optical recording

Intracellular recording can affect the passive electrical properties of neurons, which could conceivably affect their

frequency responses to applied electric fields. We therefore loaded slices with the voltage sensitive dye RH-795 and measured the membrane potential changes in the CA3c pyramidal layer. We measured responses to DC fields and AC fields at 16 and 50 Hz (Fig. 2A and B). The poor signal to noise ratio inherent in using this kind of optical measurement meant that we needed to use relatively high field strengths (150 V m^{-1} p-p) and averaging of 100

traces for each estimate. The size of the applied field (75 V m^{-1}) will activate voltage-gated currents (Bikson *et al.* 2004), explaining the time dependence evident in the response to soma-depolarizing DC (Fig. 2Ca). We therefore used the hyperpolarizing fields to estimate the time constant of the response of the membrane potential to the applied DC fields, which was a mean of $23.3 \pm 0.9 \text{ ms}$ (Figs 2Cb), close to the values found for the transmembrane potentials recorded during DC fields in the present study ($27.6 \pm 4.0 \text{ ms}$ for depolarizing fields and $22.2 \pm 4.0 \text{ ms}$ for hyperpolarizing; Fig. 2D; Student's unpaired *t* test, $P = 0.82$) and to the $22.4 \pm 3.2 \text{ ms}$ time constant from intracellular current injection. The time constant is due to the passive electrical properties of the neurons, and suggests that AC fields will be less effective than DC in altering transmembrane potential (Bikson *et al.* 2004).

The responses of the RH-795 signal to the AC fields were smaller than those to DC fields. The response to 16 Hz was significantly greater than that to 50 Hz (Student's paired *t* test: $P = 0.006$; Fig. 2Cc and d – lower traces and Fig. 3). The relative transmembrane potential sensitivities derived from the optical measurements at these two frequencies, as a fraction of that for DC fields, were close to the relationship between the corresponding electrophysiological measurements and frequency of applied field, again normalized to the response to DC fields (Fig. 3).

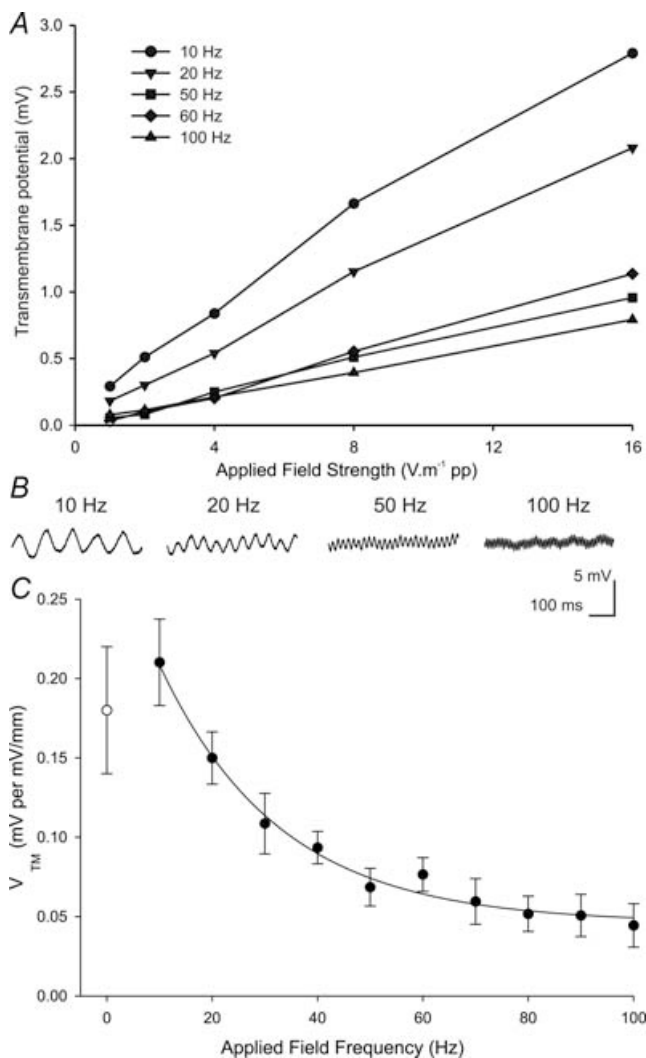


Figure 1. Effect of applied sinusoidal fields on CA3 pyramidal cells

A, transmembrane somatic potential plotted as a function of the strength of applied AC electric fields, for frequencies of 10–100 Hz (symbols given in key) reveals a near-linear relationship over the range of field strengths used here (means and standard errors of the mean of at least 6 slices). An example for a single neuron is shown in supplemental material Fig. 2B. B, recordings from one slice show that slower fields have bigger effects on transmembrane potential (also evident in the pooled data of A). C, the slope of the relationships plotted in A plotted as a function of frequency reveals an exponential decay relationship: $V_{TM} = 0.046 + 0.252e^{-0.044fq}$ ($R^2 = 0.99$; ANOVA $P < 0.0001$). The open circle to the left shows the plateau response to DC fields.

Effects of AC fields on gamma-band oscillations

The decrease in membrane response with increasing frequency of the applied fields found both by micro-electrode recording and by voltage-sensitive dyes, like the time constant for the response to DC fields, depends on the passive electrical properties of the neurons. This frequency dependence has the practical implication that AC fields at powerline frequencies will be less effective than might be predicted from DC fields. However, given the linear relationship between transmembrane potential and applied fields within the range $\pm 16 \text{ V m}^{-1}$ p-p used for this part of the study, and given the lack of a discrete threshold, the collective activities of neuronal networks may be more sensitive than expected from the changes in individual transmembrane potentials and the background noise. We therefore investigated the effects of AC fields on gamma band oscillations induced by the application of kainic acid.

Kainic acid (100 nM) applied in the circulating aCSF produced a gamma oscillation that could be recorded extracellularly within CA3 (Buhl *et al.* 1998; Vreugdenhil *et al.* 2003) with a peak power of $\sim 30 \text{ Hz}$ (31 Hz in Fig. 4). The oscillations stabilized over 30 min. After 45 min the electric fields were applied in 10 s epochs,

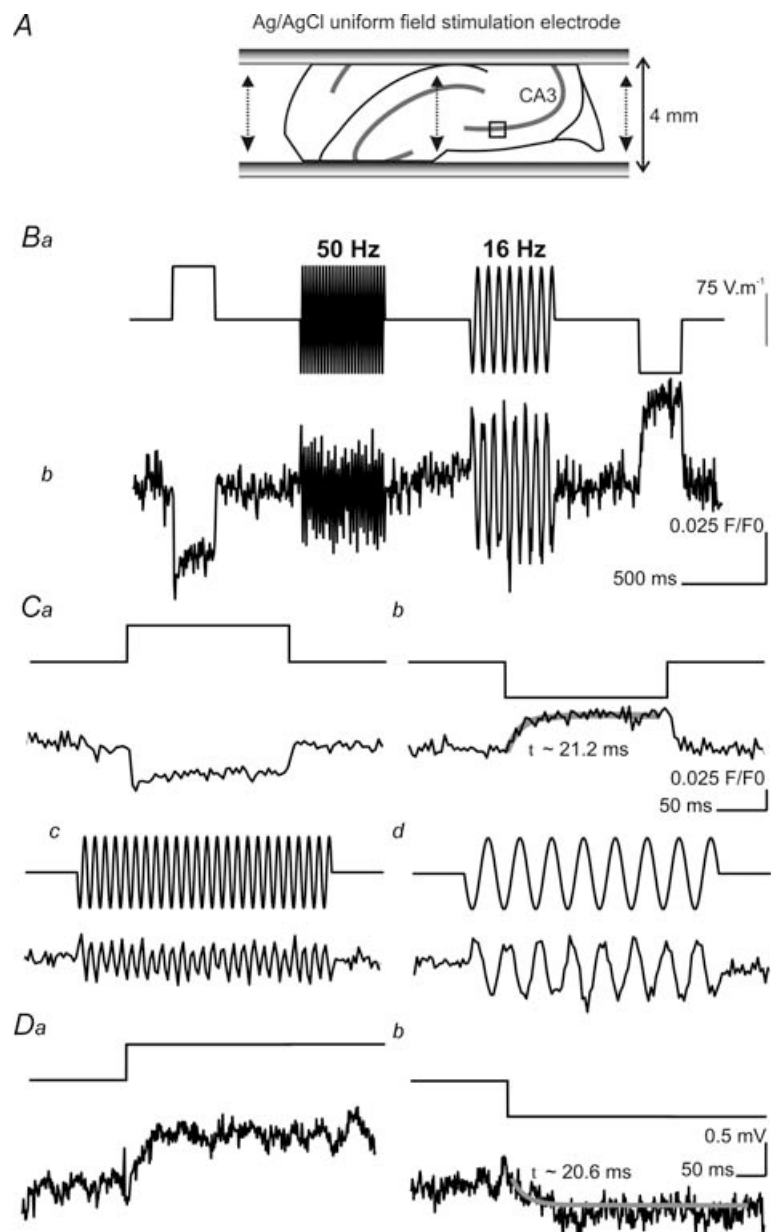
separated by 30 s, and were repeated five times for each field strength in each slice (20 times for the weaker applied fields of $\leq 2 \text{ V m}^{-1}$ p-p); the whole sequence was repeated where different frequencies were tested. Measurements were averaged over the 5 or 20 repeats. In the example shown (Fig. 4A and B), a 50 Hz, 6 V m^{-1} p-p field shifted the frequency of the peak power from 31 Hz to 26 Hz, and substantially increased the power maximum, while reducing the power at the original peak. We averaged the power spectra during the applied fields, and during equal control periods just before. Subtracting these produces a difference spectrum (Fig. 4C); the error bars represent the 95% confidence intervals for the differences between paired control and

experimental spectra, based on the pooled variance of the difference in powers at each frequency. This confirms that the increase in power centred on 25 Hz. Plotting the temporal relationship between the timing of the small negative spikes on each cycle of the biologically generated gamma oscillation and the minima of applied sinusoidal 50 Hz field (dots; Fig. 4D) reveals that the gamma cycles are locked to alternate cycles of the applied field. In cases where the control oscillation had a peak power at $< 25 \text{ Hz}$ (beta band), the increase in power centred on 17 Hz (every third cycle of the applied field).

We used Spike2 software to identify the troughs, or local minima, in the extracellular recording (Fig. 4D), and similarly the minima in the applied field. Plotting the

Figure 2. Optical measurement of membrane potential responses to extracellularly applied electric fields in the CA3 region of the hippocampus

A, hippocampal slice was stained with the voltage sensitive dye, RH-795. The slice was trimmed to remove CA1 and placed between parallel field electrodes that applied current parallel to the somato-dendritic axis of CA3c pyramidal neurons. Optical responses were monitored from a $50 \mu\text{m} \times 50 \mu\text{m}$ region of interest, centred over the pyramidal cell layer of the CA3c region (small square). B, optical signals (b, membrane depolarization decreases fluorescent intensity) from the somatic region of CA3c pyramidal neurons corresponding to transmembrane voltage responses to applied electric fields (a, 75 V m^{-1} amplitude, or 150 V m^{-1} p-p for AC fields). Optical record is the average of 100 successive sweeps. C, expansion of optical responses to the applied fields. Responses to hyperpolarizing DC fields (Cb) could be fitted by a mono-exponential decays, in this case with a time constant of 21.2 ms (grey line), comparable to those measured electrically. The depolarizing current (Ca) is complicated by substantial voltage-sensitive currents. AC field application (150 V m^{-1} p-p; c and d) was less effective at inducing voltage changes than DC fields. D, expansion of transmembrane potential change measured with sharp microelectrodes in response to depolarizing (a) and hyperpolarizing (b) field application (8 V m^{-1} ; grey curve indicates exponential fit). In this case the traces are single sweeps, which were used for fitting exponentials.



time between the gamma spikes and the applied field minima within ± 30 ms of each of the latter (x -axis in Fig. 4E) against the cycle number (y -axis) produces a 'raster plot', which in this case shows clear clustering, with the highest probability of gamma spikes 5 ms after the minima in the applied field. In this case the minima in the applied field correspond to soma hyperpolarization, so the maximal firing precedes peak soma depolarization by 5 ms, consistent with lags between pyramidal layer negativity and pyramidal cell firing found previously (Fisahn *et al.* 1998; Mann *et al.* 2005). The peri-trigger or 'event correlation' histogram confirms the distribution evident in the raster plot (Fig. 4E). The peaks in the peri-trigger histogram and raster plots are separated by 20 ms, but the period of the 25 Hz oscillation is 40 ms: this is because cycles of the applied field alternate between those that do entrain a gamma cycle and result in a lag of 5 ms, and those that do not and result in a lag of 25 ms (i.e. after the next applied field minimum). Weaker fields have less clear effects that need more sensitive analysis. We approached this in two ways: (i) assessing entrainment (measuring the association between the timing of the field minima and the gamma cycles), and (ii) measuring the differences in repeated estimates of the power spectra (Fig. 4C).

Entrainment

The null hypothesis, that there is no association between the timing of the applied sinusoid and the gamma oscillations, predicts a uniform distribution for the intervals between the minima in the applied and biological signals. In practice this can appear in the raster plot either as a uniform scatter of dots (Fig. 5B), or as a series of

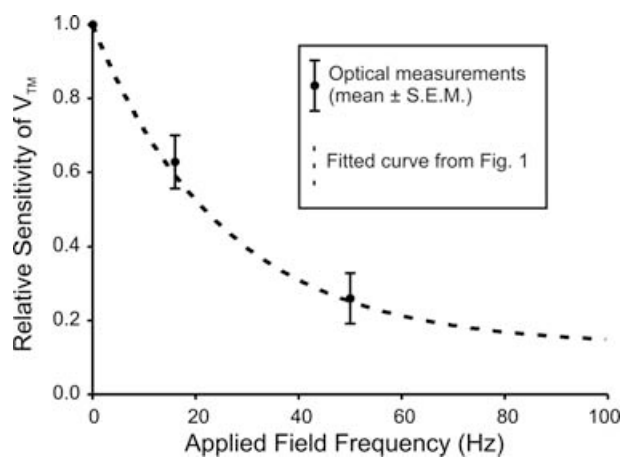


Figure 3. Comparison of optical and electrophysiological estimates of effects of applied fields

Mean \pm S.E.M. of the sensitivity of optically measured membrane potentials to AC fields at 16 and 50 Hz, normalized to that at DC, plotted on the curve relating the electrophysiological estimates of sensitivity to frequency, again normalized to the sensitivity at DC.

diagonal stripes of high dot densities (see supplemental material Fig. 4) if the applied and biological oscillations have similar frequencies but are not correlated. The uniformity of the distribution of the intervals between applied and biological oscillations can be tested using the Kolmogorov–Smirnov (KS) test (more commonly used to test for deviations from the Gaussian distribution before statistical analyses). Two examples of the effects of 1 V m^{-1} p-p, 50 Hz fields are shown in Fig. 5. This weak field can entrain the gamma oscillations (Fig. 5A). In the raster plot faint increases in density appear at fixed lags. The event correlation histogram shows clear peaks that exceed 2 standard deviations from mean calculated for control data over a period of 10 s just before the application of the 10 s long AC fields, using triggers at 20 ms intervals as surrogates for the absent AC fields; values fall outside this range $\sim 70\%$ of the time, and there is a vanishingly small probability this could occur by chance. The KS test for this case revealed a significance level of $P > 0.001$ and a Z score of 2.8. The other case illustrated (Fig. 5B) shows no evidence of association in the histogram, with $\sim 10\%$ of values outside 2 standard deviations, nor in the raster plots, where the KS test reveals $P = 0.93$ and $Z = 0.55$. Typically the significance of the KS test switches from $P > 0.8$ to $P < 0.01$ within a single step of the field strength (see supplemental material Fig. 5). Control measurements were made by generating triggers at the same frequency as the applied field, but without any polarizing current; in all cases these resulted in KS Z scores < 0.7 and $P > 0.9$.

We examined the effect of field strengths of $1\text{--}10 \text{ V m}^{-1}$ p-p at 20–50 Hz, and of 0.5 V m^{-1} p-p at 50 Hz only (see supplemental material Fig. 6). For each slice there was a clear threshold AC field required to entrain the oscillation (see supplemental material Fig. 5). AC fields $\geq 6 \text{ V m}^{-1}$ peak to peak were effective in entraining the oscillations in all slices and at all frequencies tested. Fields of 0.5 V m^{-1} p-p were effective in only 1 out of 5 cases at 50 Hz. Fields of 1 V m^{-1} p-p were effective in entraining the gamma spikes in half the cases (12/24) at 50 Hz, and nearly all at lower frequencies (e.g. 5/6 at 20 Hz): the slower applied fields were more effective in modulating the oscillations, as might be expected from their greater effects on trans-membrane potentials.

Difference spectra

Subtle changes in power spectra can be difficult to identify. We therefore calculated the means and standard deviation for each frequency within the spectra from before and during each of the five repeats of each applied field strength. We then were able to calculate the mean and standard deviation of the differences between the controls and field application. Plotting the mean difference with error bars for 95% confidence limits means that failure to overlap the zero difference line indicates a potentially significant

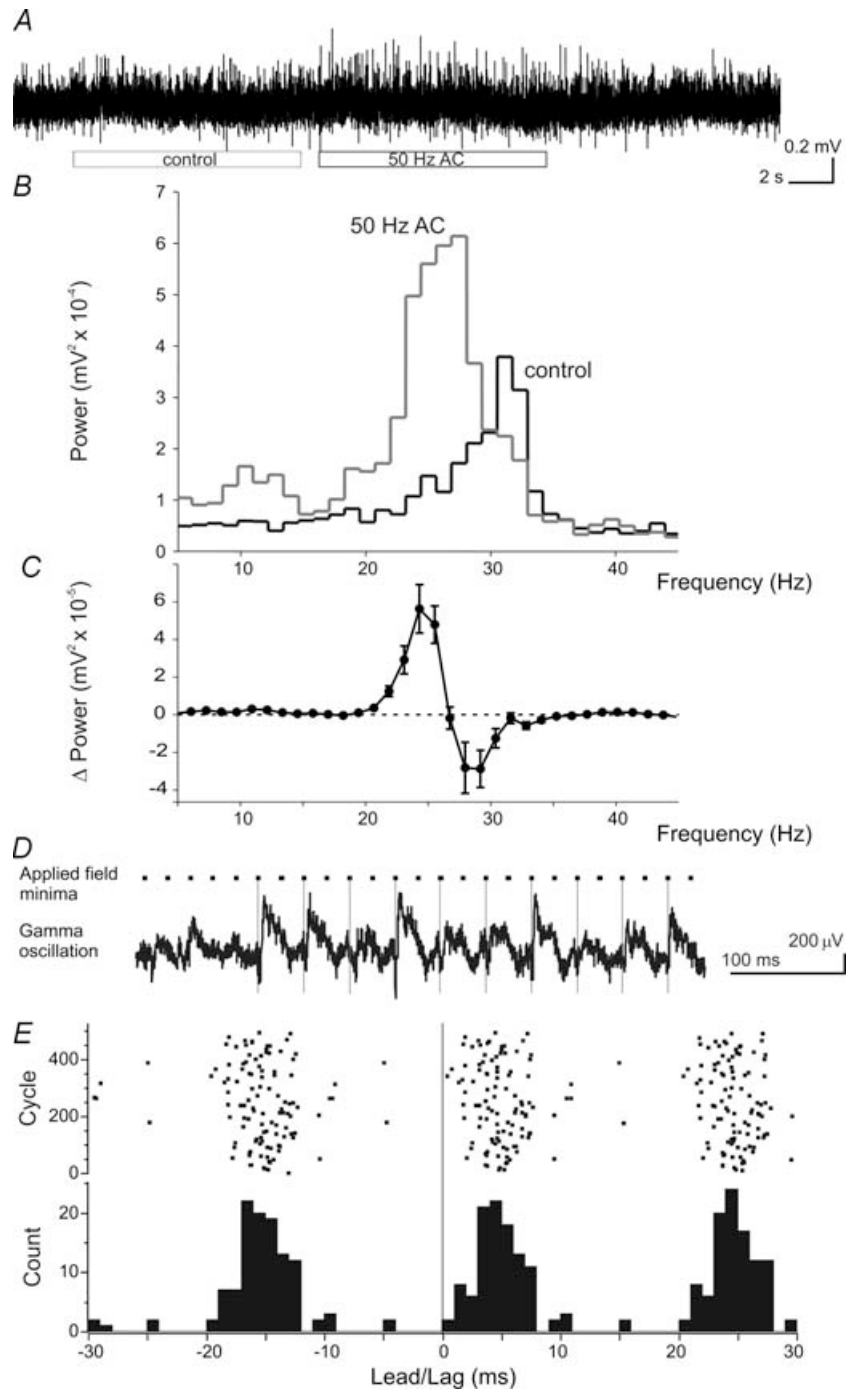


Figure 4. Effect of AC fields on kainate-induced gamma oscillations

A, field potential recording from stratum pyramidale. A 10 s duration 50 Hz electric field was applied at the time marked by the '50 Hz AC' bar. The 'control' bar indicates the period used for the control power spectrum. B, power spectra obtained by FFT for the control and applied field epochs in A. Note the shift in the peak power and frequency. C, the differences in the means (bars = 95% confidence interval) of the power spectra for five 10 s epochs with and without the applied field, showing the increase in power centred on 25 Hz during the applied field, and the decrease at the baseline gamma frequency, centred just under 30 Hz in this case. D, expanded gamma oscillation with the times of the minima in the applied field marked above; note the small negative waves on each cycle of gamma align with alternate minima of the applied field, a process we will call 'entrainment'. E, top, 'raster plot' of times of the gamma cycle minima 30 ms either side of each minimum in the applied field; successive cycles of the applied field are plotted along the y-axis. Bottom, histogram of all the spikes included in the raster plot.

result (Fig. 6). Slices differed in their sensitivity, much as indicated by the KS analysis (see supplemental material Fig. 6). The weaker fields affected some slices and not others: in the 0.5 V m^{-1} p-p 50 Hz field examples in Fig. 6A the upper plot has 3 of the 16 differences within 10 Hz of the baseline peak outside the 95% confidence interval, and has a KS Z score of 1.39, $P = 0.04$, while the lower plot, from a different slice, has a KS Z score of 0.79, $P = 0.56$. Four out of 12 slices tested at 0.5 V m^{-1} showed three or more differences outside the 95% confidence intervals within $\pm 10 \text{ Hz}$ of the baseline peak frequency. Figure 6B shows the response to increasing field strengths in a different slice. In this case there is an equivocal effect at 1 V m^{-1} p-p. At 2 V m^{-1} p-p field there is a clear shift from the baseline peak frequency of 29 Hz (clearly decreased power) to 26.5 Hz (increased power), while at 6 and 10 V m^{-1} p-p fields the gamma rhythm is locked to 25 Hz, or alternate cycles of the applied field. The corresponding KS test Z-values were, respectively, 1.1, 2.27, 3.62, and 4.96 (Fig. 6B; $P = 0.17$ for 1 V m^{-1} and < 0.001 for the stronger fields). The variation in sensitivities of slices could be due either to genuine differences in the neuronal organization in those rats, or to technical differences such as variations in the cutting angle of the slice, which could alter the lengths of dendrite preserved.

Discussion

We found that gamma rhythms induced in CA3 by 100 nM kainic acid were modulated by applied 50 Hz AC

electric fields producing potential gradients as weak as 1 V m^{-1} p-p (354 mV m^{-1} r.m.s.) in 50% of slices, and by 0.5 V m^{-1} p-p (177 mV m^{-1} r.m.s.) in 20% of slices. These voltage gradients, respectively, correspond to about 50 and 100 mA m^{-2} p-p (17 and 35 mA m^{-2} r.m.s.). The modulation took the form of a clear shift in the peak of the power spectra for fields $\geq 2 \text{ V m}^{-1}$ (708 mV m^{-1} r.m.s.) and more subtle changes in power and in entrainment of the excitatory part of the cycle for fields of $\geq 0.5 \text{ V m}^{-1}$ (177 mV m^{-1} r.m.s.). The effects on both power spectrum and spike timing depended on the frequency of the applied fields, with slower frequencies being more effective.

The applied fields altered the transmembrane potential measured at the soma by 0.18 mV per V m^{-1} for DC fields, with a time constant of 22 ms. AC fields at 50 Hz altered transmembrane potential by 0.07 mV per V m^{-1} . The effect of the AC fields, whether measured electrophysiologically or optically, depended on frequency: those at 10 Hz were similar to DC, with the size of the effect decreasing as an exponential decay function of frequency (several other functions fit the data, but this is one of the simplest and can be related to the passive properties of biological membranes). The linear relationship between applied field and induced transmembrane potential suggests that there may be no clear threshold. In contrast, the ability of applied AC fields to alter gamma oscillations did have a well-defined threshold in each slice: presumably the neuronal network switches from its endogenous frequency to the frequency paced by the AC field when the field is strong enough to add

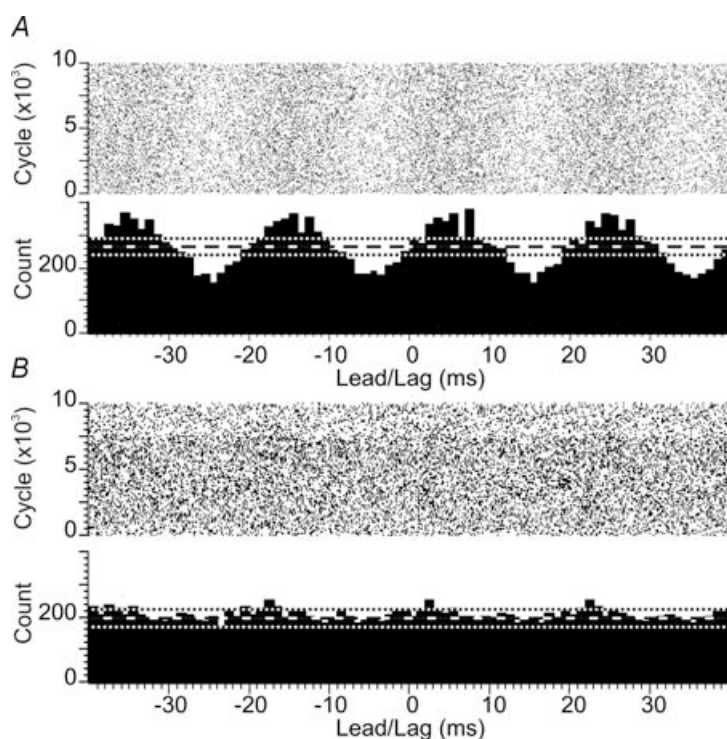


Figure 5. Raster plots of effects of weak sinusoidal fields

A, a relatively sensitive slice reveals modulation of the timing of spikes during gamma by a 1 V m^{-1} p-p AC field, both in the raster plot (above) and the histogram (below). The horizontal dashed grey line indicates the mean count (and the dotted lines ± 2 s.d., or 95% confidence interval) for similar histograms generated during control epochs preceding the applications of the fields. B, a different slice fails to reveal such a modulation, both by eye and from the Kolmogorov–Smirnov tests described in the text.

sufficient soma depolarization to the excitatory phase of the gamma oscillation to make some critical fraction of neurons fire within a few milliseconds of the peak soma depolarization. Given that only 2–5% of pyramidal cells fire during each gamma cycle (Fisahn *et al.* 1998; Mann *et al.* 2005), that critical fraction need not be large.

Previous studies of the effects of AC magnetic fields on the slower ‘theta’ oscillations induced by carbachol revealed a disruption of the network activity by 1 Hz 56 μT fields, while 60 Hz fields did not have significant effects (Bawin *et al.* 1996). The same group reported long-lasting effects of 5 Hz and 60 Hz sinusoidal electric fields on CA1 pyramidal cell excitability as measured by evoked potentials (Bawin *et al.* 1984, 1986). We found no effects outlasting the sinusoidal electric fields on evoked responses in CA1; the reason for this difference remains unclear – the field strengths were comparable, and the species was the same. In our previous work on DC fields applied to CA1 we did find longer lasting effects, but only when the fields were strong enough to trigger epileptiform activity (Bikson *et al.* 2004). The weaker fields in the present study on CA3 avoided triggering epileptiform activity. Other studies showing effects of AC fields on CA1 lasting a minute or two beyond the field application generally used much larger field strengths (100 V m^{-1} and above, intended to block epileptiform activity by increasing extracellular potassium and inducing depolarization block (Lian *et al.* 2003); the duration of the effect presumably results from the time taken for potassium to return to baseline.

Previous work on CA3 has revealed effects of weak electric fields. Francis *et al.* (2003) showed that Gaussian waveforms could trigger epileptiform bursts in slices exposed to convulsant if they were presented slightly earlier than the next expected burst. Their waveforms were 26 ms wide at half-height and had a threshold of 0.3 V m^{-1} peak (140 mV m^{-1} r.m.s.), comparable to thresholds found in the present study on the effects of continuous sinusoids on physiological oscillations. Fujisawa *et al.* (2004) found that non-uniform ~ 30 Hz fields, estimated at 5 V m^{-1} , applied to slice cultures (to simulate gamma oscillations induced by carbachol), modulated the latency of firing of CA3 pyramidal cells evoked by focal electrical stimulation.

The minimum effective fields found here are smaller than those generated by the hippocampus itself: up to 8 V m^{-1} during normal spontaneous physiological oscillations (Winson, 1974; Buzsáki *et al.* 1986; Brankack *et al.* 1993), and up to 70 V m^{-1} evoked field potentials and epileptic activity (Swann *et al.* 1986; Turner & Richardson, 1991; Bragin *et al.* 1997). This suggests that endogenous electric fields can play a role in both normal and pathological function (Jefferys, 1995).

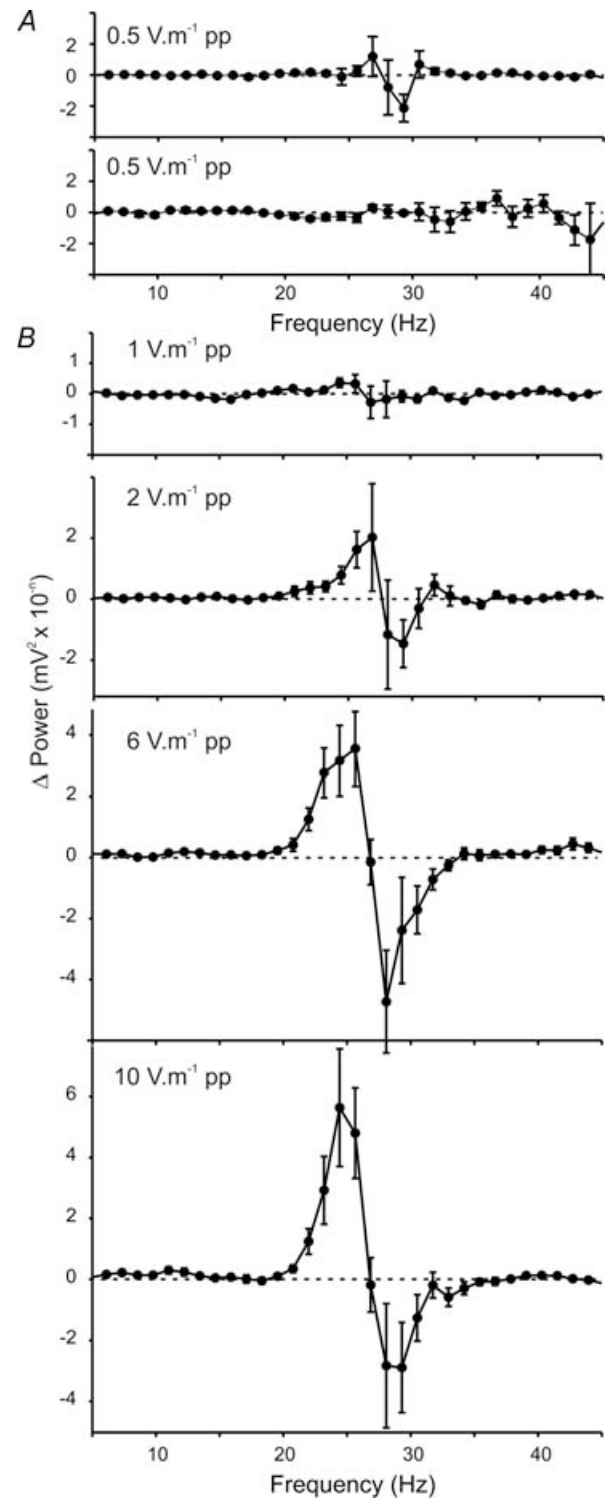


Figure 6. Difference spectra

A, difference spectra for relatively sensitive (upper spectrum) and insensitive (lower) slice exposed to a 0.5 V m^{-1} p-p 50 Hz field. B, a less sensitive slice shows no clear changes at 1 V m^{-1} p-p, but progressively more marked effects as the fields increase. Those above 6 V m^{-1} p-p show increases centred on 25 Hz, corresponding to alternate cycles of the applied field; that for 2 V m^{-1} p-p reveals a smaller shift in the frequency of the peak change. (Differences in power scaled $\times 10^{-3}$ in A, and $\times 10^{-5}$ in B.)

The frequency dependence of these phenomena has practical implications. Powerline frequencies (60 Hz in North America, 50 Hz in Europe and elsewhere) have about 0.4 times the effect of a DC field of the same amplitude. The 354 mV m^{-1} r.m.s. field found to be effective (but not necessarily deleterious) here is about 3.5 times the occupational exposure guidelines (McKinlay *et al.* 2004), and the significant effects of 177 mV m^{-1} in a minority of slices is less than double those guidelines. The slower frequencies of some traction and security systems (e.g. 16–20 Hz) had about the same effect of DC, about 3 times that for 50–60 Hz, and thus may have greater effects on brain function.

The 1 V m^{-1} p-p threshold for 50 Hz fields will induce fluctuations of $\sim 70 \mu\text{V}$ at the soma. This is considerably lower than the membrane noise analysed in depth by Jacobson *et al.* (2005), who estimated standard deviations for neocortical pyramidal cells of 190–540 μV , depending on membrane potential, comparable to our own rough estimates of s.d.: 500 μV in neocortex and 750 μV for CA3. Noise is thought to limit the sensitivity of cells to applied fields (Weaver & Astumian, 1990; Vincze *et al.* 2005). The apparent contradiction is likely to arise from the simultaneous action of the applied field to a network of neurons close to threshold and with a common orientation, so that while the induced transmembrane potentials may be undetectable in individual neurons, their simultaneous small effects suffice to increase the probability of firing across the neuronal population during the depolarizing part of the applied AC field. This has the consequence of shifting the timing of the pyramidal cell discharge and producing a statistically detectable change in the oscillation.

References

- Bawin SM, Satmary WM, Jones RA, Adey WR & Zimmerman G (1996). Extremely-low-frequency magnetic fields disrupt rhythmic slow activity in rat hippocampal slices. *Bioelectromagnetics* **17**, 388–395.
- Bawin SM, Sheppard AR, Mahoney MD, Abu-Assal M & Adey WR (1986). Comparison between the effects of extracellular direct and sinusoidal currents on excitability in hippocampal slices. *Brain Res* **362**, 350–354.
- Bawin SM, Sheppard AR, Mahoney MD & Adey WR (1984). Influences of sinusoidal electric fields on excitability in the rat hippocampal slice. *Brain Res* **323**, 227–237.
- Bikson M, Inoue M, Akiyama H, Deans JK, Fox JE, Miyakawa H & Jefferys JGR (2004). Effects of uniform extracellular DC electric fields on excitability in rat hippocampal slices in vitro. *J Physiol* **557**, 175–190.
- Bragin A, Csisvari J, Penttonen M & Buzsáki G (1997). Epileptic afterdischarge in the hippocampal-entorhinal system: current source density and unit studies. *Neuroscience* **76**, 1187–1203.
- Brankack J, Stewart M & Fox SE (1993). Current source density analysis of the hippocampal theta rhythm: associated sustained potentials and candidate synaptic generators. *Brain Res* **615**, 310–327.
- Buhl EH, Tamas G & Fisahn A (1998). Cholinergic activation and tonic excitation induce persistent gamma oscillations in mouse somatosensory cortex *in vitro*. *J Physiol* **513**, 117–126.
- Buzsáki G, Czopf J, Kondakor I & Kellenyi L (1986). Laminar distribution of hippocampal rhythmic slow activity (RSA) in the behaving rat: current-source density analysis, effects of urethane and atropine. *Brain Res* **365**, 125–137.
- Fisahn A, Pike FG, Buhl EH & Paulsen O (1998). Cholinergic induction of network oscillations at 40 Hz in the hippocampus *in vitro*. *Nature* **394**, 186–189.
- Francis JT, Gluckman BJ & Schiff SJ (2003). Sensitivity of neurons to weak electric fields. *J Neurosci* **23**, 7255–7261.
- Fujisawa S, Matsuki N & Ikegaya Y (2004). Chronometric readout from a memory trace: gamma-frequency field stimulation recruits timed recurrent activity in the rat CA3 network. *J Physiol* **561**, 123–131.
- Haas HL & Jefferys JGR (1984). Low-calcium field burst discharges of CA1 pyramidal neurones in rat hippocampal slices. *J Physiol* **354**, 185–201.
- Jacobson GA, Diba K, Yaron-Jakoubovitch A, Oz Y, Koch C, Segev I & Yarom Y (2005). Subthreshold voltage noise of rat neocortical pyramidal neurones. *J Physiol* **564**, 145–160.
- Jefferys JGR (1981). Influence of electric fields on the excitability of granule cells in guinea-pig hippocampal slices. *J Physiol* **319**, 143–152.
- Jefferys JGR (1995). Non-synaptic modulation of neuronal activity in the brain: electric currents and extracellular ions. *Physiol Rev* **75**, 689–723.
- Jefferys JGR & Haas HL (1982). Synchronized bursting of CA1 pyramidal cells in the absence of synaptic transmission. *Nature* **300**, 448–450.
- Lian J, Bikson M, Sciortino C, Stacey WC & Durand DM (2003). Local suppression of epileptiform activity by electrical stimulation in rat hippocampus *in vitro*. *J Physiol* **547**, 427–434.
- Mann EO, Suckling JM, Hajos N, Greenfield SA & Paulsen O (2005). Perisomatic feedback inhibition underlies cholinergically induced fast network oscillations in the rat hippocampus *in vitro*. *Neuron* **45**, 105–117.
- McKinlay AF, Allen SG, Cox R, Dimbylow PJ, Mann SM, Muirhead CR, Saunders RD, Sienkiewicz ZJ, Stather JW & Wainwright PR (2004). *Advice on Limiting Exposure to Electromagnetic Fields (0–300 GHz)*. Documents of the NRPB 15.2, pp. 1–35. NRPB, Chilton, UK.
- Saunders RD & Jefferys JGR (2002). Weak electric field interactions in the central nervous system. *Health Phys* **83**, 366–375.
- Swann JW, Brady RJ, Friedman RJ & Smith EJ (1986). The dendritic origins of penicillin-induced epileptogenesis in CA3 hippocampal pyramidal cells. *J Neurophysiol* **56**, 1718–1738.
- Turner RW & Richardson TL (1991). Apical dendritic depolarizations and field interactions evoked by stimulation of afferent inputs to rat hippocampal CA1 pyramidal cells. *Neuroscience* **42**, 125–135.

- Vincze G, Szasz N & Szasz A (2005). On the thermal noise limit of cellular membranes. *Bioelectromagnetics* **26**, 28–35.
- Vreugdenhil M, Jefferys JGR, Celio MR & Schwaller B (2003). Parvalbumin-deficiency facilitates repetitive IPSCs and gamma oscillations in the hippocampus. *J Neurophysiol* **89**, 1414–1422.
- Vreugdenhil M & Toescu EC (2005). Age-dependent reduction of gamma oscillations in the mouse hippocampus in vitro. *Neuroscience* **132**, 1151–1157.
- Weaver JC & Astumian RD (1990). The response of living cells to very weak electric fields: the thermal noise limit. *Science* **247**, 459–462.
- Winson J (1974). Patterns of hippocampal theta rhythm in the freely moving rat. *Electroencephalogr Clin Neurophysiol* **36**, 291–301.

Acknowledgements

The authors are grateful to the UK Department of Health and BBSRC for supporting this work, Dr Alan White (University of Birmingham) for statistical advice, Mr Greg Smith for the script to fit and remove sine waves, Dr Marom Bikson for his assistance and advice during the early stages of this work, and to Drs John Fox, Martin Vreugdenhil and Edward Tarte for helpful discussions.

Supplemental material

Online supplemental material for this paper can be accessed at: <http://jp.physoc.org/cgi/content/full/jphysiol.2007.137711/DC1> and <http://www.blackwell-synergy.com/doi/suppl/10.1113/jphysiol.2007.137711>